Intramolecular Haptotropic Rearrangements of the Tricarbonylchromium Complex in Small Polycyclic Aromatic Hydrocarbons

J. Oscar C. Jiménez-Halla,[†] Juvencio Robles,[‡] and Miquel Solà*,[†]

Institut de Química Computacional and Department de Química, Universitat de Girona, Campus de Montilivi, 17071 Girona, Catalonia, Spain, and Facultad de Química, Universidad de Guanajuato, Noria Alta s/n 36010 Guanajuato, Gto. Mexico

Received June 2, 2008

Haptotropic rearrangement reaction mechanisms for a series of polycyclic aromatic hydrocarbons (PAHs) of three and four fused six-membered rings attached to a tricarbonylchromium complex were investigated by theoretical methods. All possible ways by which haptomigrations can occur were explored, as for the less symmetric PAHs there are nonequivalent reaction pathways. The metal complex prefers to be coordinated on the less substituted rings (the more aromatic ones) and tends to avoid the migration to the more substituted ring. A paradigmatic example of this behavior is the case of triphenylene, where the coordination with the outer rings is 17.4 kcal·mol^{-1} more favored than complexation with the inner ring. The energy barriers for haptomigration vary from 16.4 (phenalene) to 24.5 kcal·mol^{-1} (triphenylene). In general, small energy differences are found between energy barriers of the so-called *exo* and *endo* pathways.

Introduction

Inter-ring haptotropic rearrangements (IRHRs) of transition-metal (TM) complexes in which the TM π-coordinated to the polycyclic aromatic hydrocarbon (PAH) migrates between different rings of the PAH have been intensively studied, both experimentally and theoretically, over the past three decades.[1−6] Although sigmatropic shifts (involving intramolecular formation/rupture of σ-bonds) were first studied, these thermally induced rearrangements became very popular for their applications in TM-mediated organic synthesis.[7−11] One of the reasons is that the interaction between the low-lying unoccupied orbitals of the TM moiety and the high-lying occupied π-orbitals of the PAH[1,12−14] results in an important charge transfer from the organic π-ligands to the TM that changes the reactivity of the PAH dramatically.[15−17] Another reason is the possibility to use IRHRs in the design of molecular switches.[18−21]

There are two kinds of haptotropic migrations: intramolecular (when the metal fragment changes its coordination site through the same π-face of the hydrocarbon ligand) and intermolecular (i.e., the metallic complex migrates from one molecule to another, usually by means of a coordinating solvent helping as an intermediate). The focus of the present study is on the intramolecular IRHRs because these haptotropic rearrangements

* Corresponding author. Tel: +34.972.41.89.12. Fax: +34.972.41.83.56. E-mail: miquel.sola@udg.es.
[†] Universitat de Girona.
[‡] Universidad de Guanajuato.

(1) Albright, T. A.; Hofmann, P.; Hoffmann, R.; Lillya, C. P.; Dobosh, P. A. *J. Am. Chem. Soc.* **1983**, *105*, 3396.
(2) Deubzer, B.; Fritz, H. P.; Kreiter, C. G.; Öfele, K. *J. Organomet. Chem.* **1967**, *7*, 289.
(3) Kündig, E. P.; Desobry, V.; Grivet, C.; Rudolph, B.; Spichiger, S. *Organometallics* **1987**, *6*, 1173.
(4) Muetterties, E. L.; Bleeke, J. R.; Wucherer, E. J.; Albright, T. A. *Chem. Rev.* **1982**, *82*, 499.
(5) Muller, J.; Goser, P.; Elian, M. *Angew. Chem., Int. Ed. Engl.* **1969**, *8*, 374.
(6) Rogers, R. D.; Atwood, J. L.; Albright, T. A.; Lee, W. A.; Rausch, M. D. *Organometallics* **1984**, *3*, 263.
(7) Arrais, A.; Diana, E.; Gervasio, G.; Gobetto, R.; Marabello, D.; Stanghellini, P. L. *Eur. J. Inorg. Chem.* **2004**, 1505.
(8) Dötz, K. H.; Szesni, N.; Nieger, M.; Nattinen, K. *J. Organomet. Chem.* **2003**, *671*, 58.
(9) Longen, A.; Nieger, M.; Airola, K.; Dötz, K. H. *Organometallics* **1998**, *17*, 1538.
(10) Ochertyanova, E. A.; Hansen, H. J.; Ustynyuk, Y. A. *Helv. Chim. Acta* **2002**, *85*, 1166.
(11) Oprunenko, Y. F.; Akhmedov, N. G.; Laikov, D. N.; Malyugina, S. G.; Mstislavsky, V. I.; Roznyatovsky, V. A.; Ustynyuk, Y. A.; Ustynyuk, N. A. *J. Organomet. Chem.* **1999**, *583*, 136.
(12) Dötz, K. H.; Stinner, C.; Nieger, M. *J. Chem. Soc., Chem. Commun.* **1995**, 2535.
(13) Kirss, R. U.; Treichel, P. M. *J. Am. Chem. Soc.* **1986**, *108*, 853.
(14) Oprunenko, Y. F.; Reshetova, M. D.; Malyugina, S. G.; Ustynyuk, Y. A.; Ustynyuk, N. A.; Batsanov, A. S.; Yanovsky, A. I.; Struchkov, Y. T. *Organometallics* **1994**, *13*, 2284.
(15) Hubig, S. M.; Lindeman, S. V.; Kochi, J. K. *Coord. Chem. Rev.* **2006**, *200−202*, 831.
(16) Merlic, C. A.; Zechman, A. L.; Miller, M. M. *J. Am. Chem. Soc.* **2001**, *123*, 11101.
(17) Suresh, C. H.; Koga, N.; Gadre, S. R. *Organometallics* **2000**, *19*, 3008.
(18) Jahr, H. C.; Nieger, M.; Dötz, K. H. *Chem. Commun.* **2003**, 2866.
(19) Jahr, H. C.; Nieger, M.; Dötz, K. H. *J. Organomet. Chem.* **2002**, *641*, 185.
(20) Jahr, H. C.; Nieger, M.; Dötz, K. H. *Chem.−Eur. J.* **2005**, *11*, 5333.
(21) Pan, J.; Kampf, J. W.; Ashe, A. J. *Organometallics* **2006**, *25*, 197.
(22) Dötz, K. H.; Wenzel, B.; Jahr, H. C. *Chromium-Templated Benzannulation and Haptotropic Metal Migration*; Springer-Verlag: Berlin, 2004; Vol. 248, p 63.
(23) Seiders, T. J.; Baldridge, K. K.; O'Connor, J. M.; Siegel, J. S. *Chem. Commun.* **2004**, 950.
(24) Kamikawa, K.; Nishino, K.; Sakamoto, T.; Kinoshita, S.; Matsuzaka, H.; Uemura, M. *J. Organomet. Chem.* **2007**, *692*, 678.
(25) Kirillov, E.; Kahlal, S.; Roisnel, T.; Georgelin, T.; Saillard, J.-Y.; Carpentier, J.-F. *Organometallics* **2008**, *27*, 387.
(26) Nagashima, H.; Fukahori, T.; Nobata, M.; Suzuki, A.; Nakazawa, M.; Itoh, K. *Organometallics* **1994**, *13*, 3427.
(27) Niibayashi, S.; Matsubara, K.; Haga, M.; Nagashima, H. *Organometallics* **2004**, *23*, 635.

10.1021/om800505j CCC: $40.75
Publication on Web 09/25/2008

present interesting stereospecific regioselectivities during the course of some reactions.[22−24]

In most of the cases, experimental results in this area are obtained for chromium tricarbonyl complexes; however, intramolecular IRHRs have also been described for Fe,[25−27] Mo,[28] Ir,[29] Ru,[30−32] Mn,[33] and Ni,[34] and so far in organolanthanoid chemistry for Yb[35] among others. First examples of intramolecular IRHRs of the $Cr(CO)_3$ complex established the possibility to control the position of the metal tripod on a specific ring of the arene by varying the temperature conditions (usually within 70−120 °C) and the substituents.[36−38] Usually, the most stable isomer is obtained when the metal complex is attached to the least-substituted ring, which is normally the most aromatic one.[39] Moreover, the distribution of the electron density through the π-system slightly displaces the site of coordination of the metal going from a perfect η^6-complex to a reduced η^3- or η^4-species depending on the overlaps between frontier orbitals of the PAH and the tricarbonylchromium complex. This change in hapticity is called ring slippage and plays a central role for understanding the IRHRs.[29,40]

Ever since the proposal from Dötz and co-workers that the possible design of organometallic molecular switches through selective IRHRs under appropriate photothermic and/or pH-acidity reaction conditions,[18] the interest in controlling the regiochemistry of the products has grown. Some works concerning these reversible haptotropic rearrangements of a $Cr(CO)_3$ fragment along fused arene skeletons have been reported.[18−21] Particularly, the reaction mechanism of IRHRs has been debated in order to understand the fluxional nature of these organometallic compounds and the interaction of the π-electron distribution with the metal center, affecting the stability of PAHs. Some decades ago, Albright and co-workers[1,36] elucidated, by scanning potential energy surfaces (PES) with extended Hückel calculations, the possible reaction pathways for the haptomigration of the $M(CO)_n$ fragment (M = Cr, Fe, Co, Pt, Rh, and Ni and n = 2 and 3) on some bicyclic polyene systems. They suggested that the metal complex does not follow the least motion path, but rather proceeds along the ligand periphery. Recently, we have reported on the IRHR of four PAHs sharing a common naphthalenic skeleton and having different sizes and curvatures. Our results showed that the IRHR is disfavored in small and curved PAHs. Two reaction pathways were found for haptotropic migrations in these four PAHs; one mechanism involves an intermediate between two transition states connecting the hapto isomers and the second involves just one transition state following the reaction coordinate.[41]

Scheme 1. Polycyclic Aromatic Hydrocarbons Studied in This Work, Together with the Labels for the Different Rings[a]

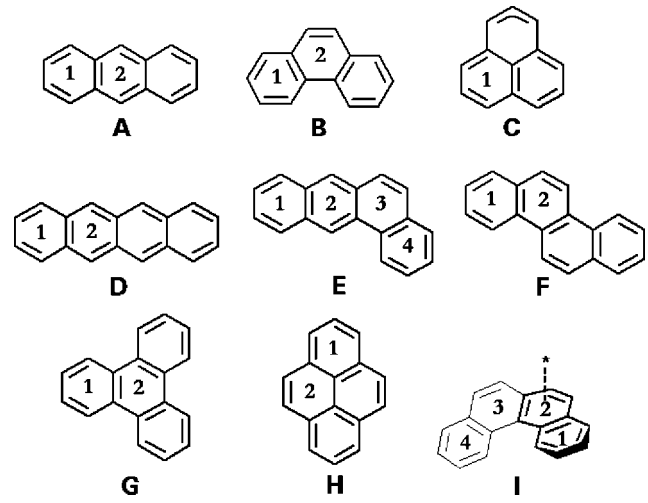

[a] The asterisk sign in nonplanar compound **I** indicates the side that was considered for the analysis of the interaction with the $Cr(CO)_3$ unit.

For the smallest acenes, as in naphthalene or anthracene, there is a single reaction pathway for the IRHR. However, for kinked benzenoid molecules, the possibility of more than a single reaction path emerges. Thus, the present study explores the different pathways for IRHRs in all PAH isomers having three and four fused six-membered rings (6-MRs) through density-functional theory (DFT) calculations. We aim at five objectives: (i) to determine the binding energy of $Cr(CO)_3$ to the series of PAHs studied; (ii) to analyze whether the arene-$Cr(CO)_3$ π-interactions are more or less favored when going from linear to kinked benzenoids of similar size; (iii) to confirm that these π-interactions are less stabilizing as the size of the PAH increases;[42−44] (iv) to find the most favorable reaction pathway for the IRHRs in the PAHs studied; and finally (v) to compare the IRHR reaction pathways and energy barriers for linear and kinked isomers.

Results and Discussion

The reaction mechanisms of intramolecular IRHRs in the benzenoid PAHs of three and four fused 6-MRs depicted in Scheme 1 have been analyzed. All benzenoid compounds considered in this study have a closed-shell singlet ground state, except phenalene (**C**), for which the ground state is a doublet. For the geometry optimizations and calculation of energy barriers, we have employed the B3LYP hybrid functional and a mixed basis set (for further information, see the Computational Details section). Naphthalene was already studied in our previous work with exactly the same methodology.[41] In that work, it was proved that this methodology provides excellent geometries for the $(\eta^6\text{-}C_{10}H_8)Cr(CO)_3$ complex as well as

(28) Zhu, G.; Janak, K. E.; Figueroa, J. S.; Parkin, G. *J. Am. Chem. Soc.* **2006**, *128*, 5452.
(29) Crabtree, R. H.; Parnell, C. P. *Organometallics* **1984**, *3*, 1727.
(30) Herbert, D. E.; Tanabe, M.; Bourke, S. C.; Lough, A. J.; Manners, I. *J. Am. Chem. Soc.* **2008**, *130*, 4166.
(31) Matsubara, K.; Oda, T.; Nagashima, H. *Organometallics* **2001**, *20*, 881.
(32) Matsubara, K.; Mima, S.; Oda, T.; Nagashima, H. *J. Organomet. Chem.* **2002**, *650*, 96.
(33) Rerek, M. E.; Basolo, F. *Organometallics* **1984**, *3*, 647.
(34) Stanger, A.; Vollhardt, K. P. C. *Organometallics* **1992**, *11*, 317.
(35) Berg, D. J.; Sun, J. L.; Twamley, B. *Chem. Commun.* **2006**, 4019.
(36) Silvestre, J.; Albright, T. A. *J. Am. Chem. Soc.* **1985**, *107*, 6829.
(37) Uebelhart, P.; Linden, A.; Hansen, H. J.; Ustynyuk, Y. A.; Trifonova, O. A.; Akhmedov, N. G.; Mstislavsky, V. I. *Helv. Chim. Acta* **1999**, *82*, 1930.
(38) Ustynyuk, Y. A.; Trifonova, O. I.; Oprunenko, Y. F.; Mstislavskiy, V. I.; Gloriozov, I. P.; Ustynyuk, N. A. *Organometallics* **1990**, *9*, 1707.
(39) Güell, M.; Poater, J.; Luis, J. M.; Mó, O.; Yáñez, M.; Solà, M. *ChemPhysChem* **2005**, *6*, 2552.
(40) Veiros, L. F. *Organometallics* **2000**, *19*, 5549.
(41) Jiménez-Halla, J. O. C.; Robles, J.; Solà, M. *J. Phys. Chem. A* **2008**, *112*, 1202; erratum **2008**, *112*, 7310.
(42) Dötz, K. H.; Stendel, J.; Müller, S.; Nieger, M.; Ketrat, S.; Dolg, M. *Organometallics* **2005**, *24*, 3219.
(43) Howell, J. A. S.; Ashford, N. F.; Dixon, D. T.; Kola, J. C.; Albright, T. A.; Kang, S. K. *Organometallics* **1991**, *10*, 1852.
(44) Al-Takhin, G.; Connor, J. A.; Skinner, H. A.; Zafarani-Moattar, M. T. *J. Organomet. Chem.* **1984**, *260*, 189.

Table 1. Distances from Cr to the Center of the Coordinated Ring, *l*, and Ring Slippage, *d* (in Å), for All the Studied Haptoisomers of Each PAH Shown in Scheme 1

	A		B		C	D	
	1	2	1	2	1	1	2
l	1.789	1.811	1.756	1.844	1.830	1.800	1.820
d	0.207	0.051	0.127	0.069	0.195	0.253	0.080

	E				F	
	1	2	3	4	1	2
l	1.795	1.803	1.868	1.771	1.780	1.819
d	0.204	0.059	0.148	0.137	0.137	0.061

	G		H		I			
	1	2	1	2	1	2	3	4
l	1.766	1.885	1.796	1.849	1.779	1.824	1.831	1.791
d	0.120	0.000	0.056	0.109	0.077	0.063	0.172	0.091

acceptable binding energies and energy barriers. The results obtained in this previous work for naphthalene (binding energy −39.26 kcal·mol^{-1} and IRHR energy barrier 23.40 kcal·mol^{-1}) will be used together with those obtained in the present study to discuss trends along the acene series.

The geometrical distances that characterize better the physical interaction between the tricarbonylchromium complex and the π-system of the studied PAHs are displayed in Table 1. It can be easily noted that the shorter distances from chromium to the coordinated ring (*l*) are those at the outer rings, indicating a stronger π-interaction of the metal complex with the less substituted rings (*vide infra*). The ring slippage displaces the $Cr(CO)_3$ tripod from the perfect η^6-coordination. This effect in the (η^6-$C_{10}H_8$)$Cr(CO)_3$ species has been discussed before by some authors[1,28,41] and has been also reported in other complexes.[40,43,45] The slippage in (η^6-$C_{10}H_8$)$Cr(CO)_3$ of 0.18 Å[41] was justified by the presence of a node at the central bonding in the HOMO and HOMO−3 orbitals of naphthalene, but also steric effects play a role.[1,28,41] The value of the slippage found in our studied systems is listed in Table 1. Interestingly, the ring slippage is, in general, more pronounced for the outer rings. This can be explained by the shape of frontier molecular orbitals (MOs) and the influence of steric effects. Thus interaction of high occupied molecular orbitals (HOMOs) with nodes at the junctions of the rings (slipping the metal to get a maximum overlap with the other nonjunctioned atoms) or antibonding interactions in these junctions (which increase the slippage even more) both increase the slippage and reduce the π-bonding interaction.[28] However, for pyrene and tetrahelicene the ring slippage is larger for one of the inner rings than for the outer ones. Pyrene possesses a HOMO with a central node between inner rings 2 (see Scheme 1). In addition, repulsive steric interactions suffered by the staggered *endo* conformation of $Cr(CO)_3$ adopted in these rings[41] decrease due to ring slippage. In the case of tetrahelicene, the central ring 3 presents the major ring slippage because of steric effects with the upper ring and the presence of a HOMO−1 with a node in the 3−4 ring junction and an antibonding interaction in the other junction. The ring slippage of the most stable (η^6-PAH)$Cr(CO)_3$ isomer, which corresponds to complexation with the outer ring, increases steadily along the series naphthalene < anthracene < tetracene, the same order followed by the binding energy (*vide infra*). It is worth noting that when comparing the ring slippage of the most stable isomer for linear and kinked benzenoids of the same size, the slippage is more important in the linear species (compare anthracene and phenanthrene or tetracene with tetraphene and chrysene).

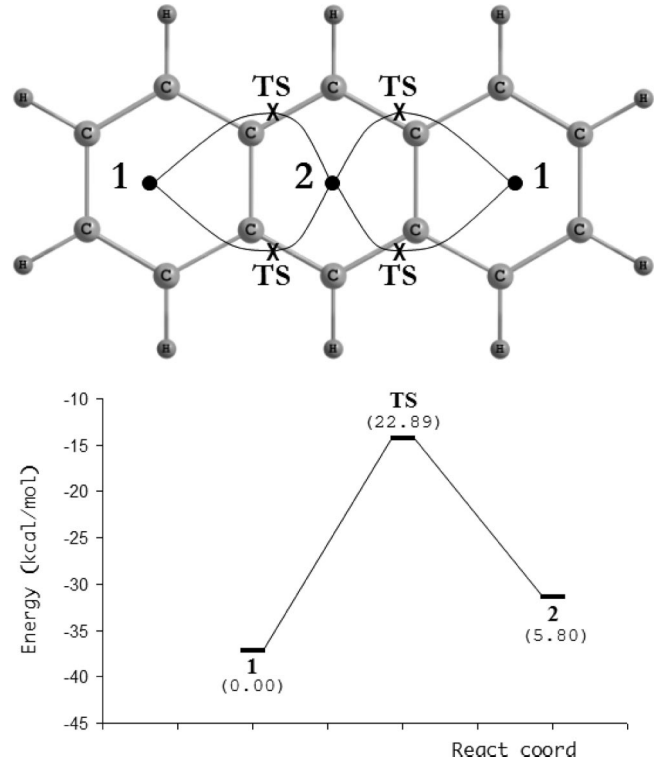

Figure 1. Sketched route for the haptotropic migration in anthracene obtained at the B3LYP/(Watchers' basis/6-31G(d,p)) level of theory (top). The labels are marked in the outlined route as black circles for minima and × for transition states (TS). Relative energies with respect to species **1** (bottom) are given in parentheses. Energy scale in the *y* axis represents binding energies corrected by BSSE with respect to isolated $Cr(CO)_3$ and anthracene. All energies are given in kcal·mol^{-1}.

In the following we present the reaction mechanisms studied, where we discuss all intermediate and transition state (TS) structures involved in each IRHR mechanism. The reader is referred to the Supporting Information for figures of the located stationary points omitted here for the sake of conciseness.

Polycyclic Aromatic Hydrocarbons Having Three Fused 6-MRs. Our target haptotropic rearrangements were investigated first in PAHs having three fused 6-MRs, namely, anthracene (D_{2h}, ^1A_g), phenanthrene (C_{2v}, $^1A_1$), and phenalene (D_{3h}, $^2A_1''$). For the former, the sketched reaction mechanism is shown in Figure 1. This is the system of this series with less different intermediates and TSs due to its high symmetry, and for this species, only two equivalent reaction pathways were found on the PES. The binding energy of the $Cr(CO)_3$ to anthracene in **1** is −37.2 kcal·mol^{-1}, about 2 kcal·mol^{-1} smaller than that of naphthalene. The relative energy of the local minimum **2** with respect to the global minimum **1** is 5.8 kcal·mol^{-1}. This difference in binding energy must be attributed to larger steric effects in **2** together with a slightly smaller π-electron density of the inner rings in anthracene.[39] Rotation of the tripod by 60° about its local approximate C_3 axis in **1** and **2** generates other stable conformers higher in energy that will not be analyzed in the present work. Indeed, in this kind of complex the extremely low rotational barriers make the rotational movement of the

(45) Calhorda, M. J.; Veiros, L. F. *Coord. Chem. Rev.* **1999**, *186*, 37.
(46) Low, A. A.; Hall, M. B. *Int. J. Quantum Chem.* **2000**, *77*, 152.
(47) Baldridge, K. K.; Siegel, J. S. *J. Phys. Chem.* **1996**, *100*, 6111.

Scheme 2. Simplified Molecular Orbital Diagram Illustrating the Interaction of Tricarbonylchromium with Anthracene[a]

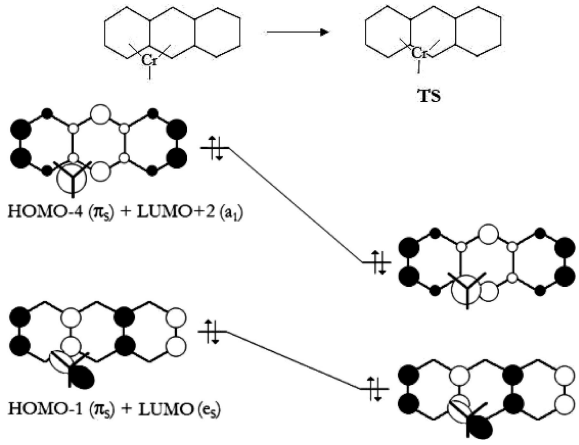

[a] The transition state somewhat slipped (right) from the exact η^3-position (left) is favored due to better overlap.

$Cr(CO)_3$ tripod basically free.[46−48] Throughout this work, we will discuss only the most stable rotational conformer. The TS for the transformation between **1** and **2** is an η^2- instead of an η^3-species judging from the shortest Cr−C distances of 2.24, 2.45, and 2.72 Å found in this TS. During the transit from **1** to the TS, the $Cr(CO)_3$ tripod rotates by about 30°. We were unable to find a first-order saddle point (a true TS) corresponding to the least motion path where the $Cr(CO)_3$ unit passes through the center of the C−C bond junction. This path, which goes through a second-order saddle point, has to surmount a large energy barrier for the same reasons discussed by Albright and co-workers in naphthalene.[1] The same authors also explained the reasons for the tripod rotation in the pathway from the reactants to the TS of the IRHR.[1] Note that, dividing the system by an imaginary line across the C−C bond junction where the $Cr(CO)_3$ migration takes place, the $Cr(CO)_3$ moiety in the TS is positioned closer to the two-ring half rather than the one-ring half. This is because the HOMO–4 (π_s) and HOMO−1 (π_s) are more localized over the central carbon atoms of the inner ring, allowing a better overlap with the LUMO+2 (a_1) and LUMO (e_s) of the metal tripod, respectively, and displacing toward it for the TS structure (see Scheme 2). On the other hand, the calculated value for the energy barrier of 22.9 kcal·mol^{-1} is slightly lower than that found for naphthalene (23.4 kcal·mol^{-1}) but relatively high when compared with that reported experimentally by Stanger and Vollhardt (SV) in the related (η^6-anthracene){bis(trialkylphosphine)nickel} species (13.6 kcal·mol^{-1}).[34] Nevertheless, SV suggested the same favored route "walk around the π system" and also the same preference of the nickel complex for the coordination to the outer rings as those found by us.

In Figure 2, the possible routes of reaction for IRHRs in phenanthrene are depicted. The binding energy for the complexation of the $Cr(CO)_3$ unit to phenanthrene in **1** is −38.1 kcal·mol^{-1}, the binding in phenanthrene being about 1 kcal·mol^{-1} stronger than in anthracene. Particularly, this system was already investigated by Dötz and co-workers with the BP86 functional.[42,49] The geometries of located stationary points and the reaction pathways reported by these authors are in perfect agreement with those found by us. The authors concluded that

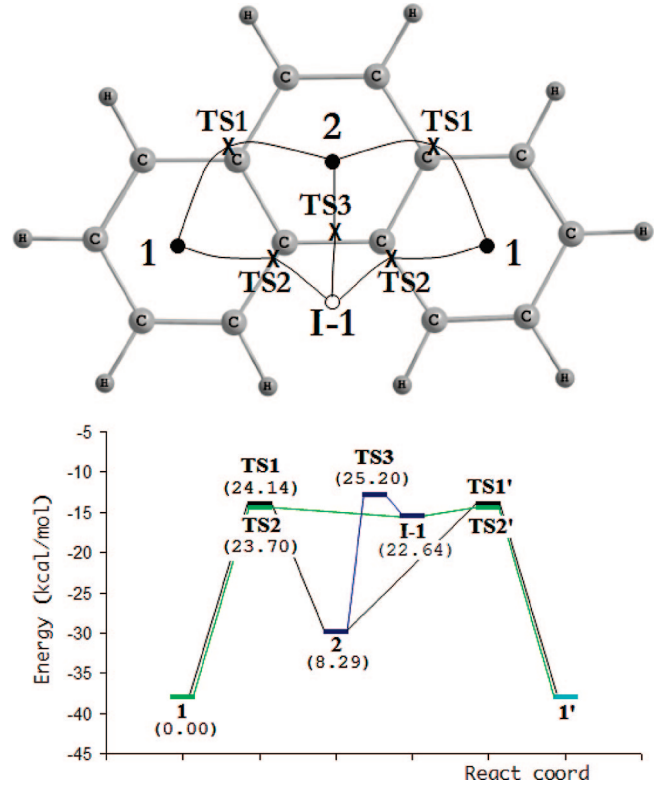

Figure 2. Sketched route for the haptotropic migrations in phenanthrene obtained at the B3LYP/(Watchers' basis/6-31G(d,p)) level of theory (top). The labels are marked in the outlined route as black circles for minima and × for transition states (TS). Relative energies with respect to species **1** (bottom) are given in parentheses. Energy scale in the *y* axis represents binding energies corrected by BSSE with respect to isolated $Cr(CO)_3$ and phenanthrene. All energies are given in kcal·mol^{-1}.

the longer pathway (along the outer periphery of the phenanthrene ligand, hereafter referred as *exo*) has a slightly higher activation energy, 30.5 kcal·mol^{-1}(24.1 kcal·mol^{-1}, our value), than the shorter pathway (along the bay region, hereafter referred as *endo*), 29.2 kcal·mol^{-1} (23.7 kcal·mol^{-1}, our value). [42] In line with their results,[42] we also found that coordination to the inner ring leads to a less stable isomer (B3LYP: 8.3 kcal·mol^{-1}; BP86: 8.2 kcal·mol^{-1}) than complexation with the more aromatic outer ring because of the reduced π-electron density and aromaticity of the central ring.[39,50] The existence of an intermediate, **I-1**, which is 22.6 kcal·mol^{-1} higher in energy than minimum **1**, is a striking difference between anthracene and its angular isomer. The presence of this intermediate can be justified from the interactions of the degenerate LUMO (e_s) and LUMO+1 (e_a) orbitals of the $Cr(CO)_3$ moiety with the HOMO−3 (π_s) and HOMO−1 (π_a) of the arene ligand, given in that order (see Scheme 3). For species like phenanthrene, this slight difference in bonding entails a temporal stabilization of this 16-electron η^4-arene-$Cr(CO)_3$ species. The orbital interactions shown in Scheme 3 also support the explanation of the possible migration to every ring by means of η^2-transition states. Moreover, the η^2-transition state (**TS3**, see Figure S2 in the Supporting Information) connecting this intermediate and minimum **2** is only 1.5 kcal·mol^{-1} higher than **TS2**, indicating that migrations through **I-1** from ring **1** to ring **1** or ring **2** have almost the same energy requirements. The most favorable IRHR

(48) Elass, A.; Brocard, J.; Surpateanu, G.; Vergoten, C. *J. Mol. Struct. (THEOCHEM)* **1999**, *466*, 35.
(49) Ketrat, S.; Muller, S.; Dolg, M. *J. Phys. Chem. A* **2007**, *111*, 6094.
(50) Portella, G.; Poater, J.; Bofill, J. M.; Alemany, P.; Solà, M. *J. Org. Chem.* **2005**, *70*, 2509; erratum, **2005**, *70*, 4560.

Scheme 3. Simplified Picture of Some Molecular Orbital Interactions of Tricarbonylchromium with Phenanthrene[a]

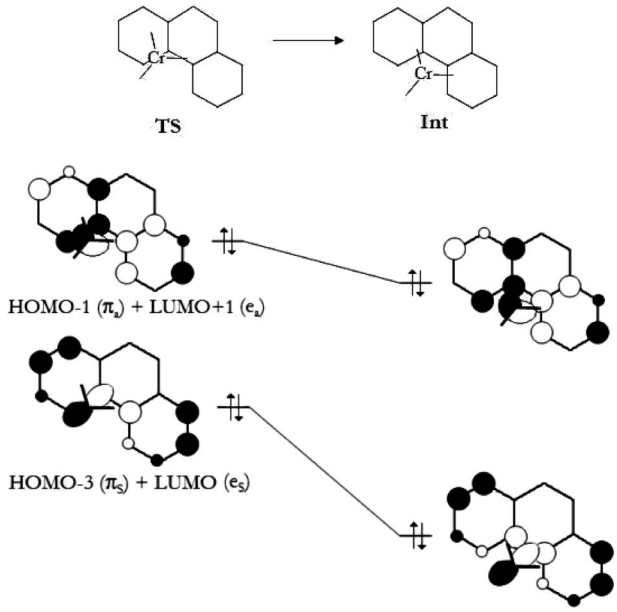

[a] The η^4-intermediate species (**Int**, right) are partially stabilized because of a good overlap with all the *endo* carbons.

pathway in phenanthrene connecting minima **1** and **2** has an energy barrier of 23.7 kcal·mol^{-1}, just slightly larger from that found in linear anthracene (22.9 kcal·mol^{-1}).

Phenalene chemistry possesses also a high experimental interest due to its three fused benzenoid rings, where alkenyl insertion reactions can be observed.[51] In this report, we have explored the PES of the neutral (phenalene)Cr(CO)$_3$ complex (doublet spin state), which has been described to be a stable complex involved in a series of addition reactions.[52] The binding energy of the Cr(CO)$_3$ to phenalene in **1** is −35.7 kcal·mol^{-1}. The possible IRHR reaction mechanisms are shown in Figure 3. Since this species shows the HOMO with a distributed electron density over the three nonjunctioned carbons of each ring, there is a significant ring slippage, but, more interestingly, it favors the "outside" haptomigration rather than through the central hinge carbon. Note that the TS structure is very similar to that found for naphthalene (see Figure S3 in the Supporting Information). The required energy for this conversion is 16.4 kcal·mol^{-1}, whereas for the other route, where there is an η^1-intermediate 24.9 kcal·mol^{-1} energetically higher with respect to structure **1**, it is more than 8 kcal·mol^{-1} disfavored. The same observation was made by Albright et al.[1] some years ago using the extended-Hückel method. Experimental data for (phenalenium(+))Cr(CO)$_3$ complexes reveal energy barriers ranging from 22.8 ± 4.1 to 23.7 ± 3.5 kcal·mol^{-1} for the haptotropic rearrangement in these compounds,[53,54] while for (phenalenide(−))Yb(L$_2$), the reported value for the IRHR energy barrier is ca. 10 kcal·mol^{-1}.[35] Although the experimental data

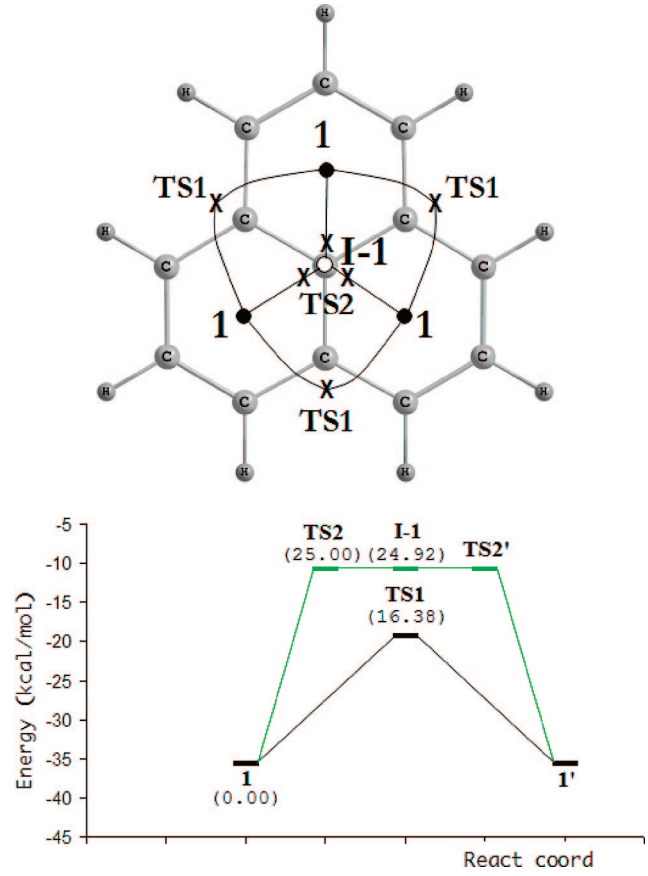

Figure 3. Sketched route for the haptotropic migrations in phenalene obtained at the B3LYP/(Watchers' basis/6-31G(d,p)) level of theory (top). The labels are marked in the outlined route as black circles for minima and × for transition states (TS). Relative energies with respect to species **1** (bottom) are given in parentheses. Energy scale in the *y* axis represents binding energies corrected by BSSE with respect to isolated Cr(CO)$_3$ and phenalene. All energies are given in kcal·mol^{-1}.

do not correspond to the system studied here, the energy barriers reported are not far from the 16.4 kcal·mol^{-1} obtained in this work.

Polycyclic Aromatic Hydrocarbons Having Four Fused 6-MRs. We have studied the haptotropic reaction mechanisms in most of the possible PAHs with four fused 6-MRs, namely, naphthacene (D_{2h}, ^1A_g, commonly referred as tetracene), tetraphene (C_s, $^1A'$), chrysene (C_{2h}, ^1A_g), pyrene (D_{2h}, ^1A_g), triphenylene (D_{3h}, $^1A_1'$), and tetrahelicene (C_2, ^1A). Migration on naphthacene is drawn in Figure 4 (see also Figure S4 for further details). The preferred coordination position of the metal tripod is at the outer rings, **1**, with a binding energy of −35.3 kcal·mol^{-1} (somewhat smaller than those of naphthalene and anthracene). Complexation to the central rings, **2**, has a binding energy that is lower by 4.9 kcal·mol^{-1}. The TSs involved in IRHRs in this species are **TS1**, which resembles that found for anthracene, and **TS2**, which is similar to that corresponding to naphthalene.[41] The energy barrier of **TS1** (22.6 kcal·mol^{-1}) is 1.2 kcal·mol^{-1} higher than that for **TS2**, and both are lower than those found for anthracene and naphthalene (*vide supra*). In fact we can say that, by comparing the series of acenes from two to four fused 6-MRs, as the system adds more rings, the binding energy decreases and the haptotropic rearrangements become energetically more feasible. These conclusions are in line with previous results showing that arene-Cr(CO)$_3$ π-interactions are less stabilizing as the size of the PAH increases.[41−44]

(51) Lin, S.; Boudjouk, P. *J. Organomet. Chem.* **1980**, *187*, C11.
(52) Murata, I. *Topics in Nonbenzenoid Aromatic Chemistry*; Hirokawa: Tokyo, 1976; Vol. 1, p 159.
(53) Akhmedov, N. G.; Katsman, E. A.; Malyugina, S. G.; Mstislavsky, V. I.; Oprunenko, Y. F.; Roznyatovsky, V. A.; Ustynyuk, Y. A.; Batsanov, A. S.; Ustynyuk, N. A. *Russ. Chem. Bull.* **1997**, *46*, 1769.
(54) Akhmedov, N. G.; Malyugina, S. G.; Mstislavsky, V. I.; Oprunenko, Y. F.; Roznyatovsky, V. A.; Batsanov, A. S.; Ustynyuk, N. A. *Organometallics* **1998**, *17*, 4607.

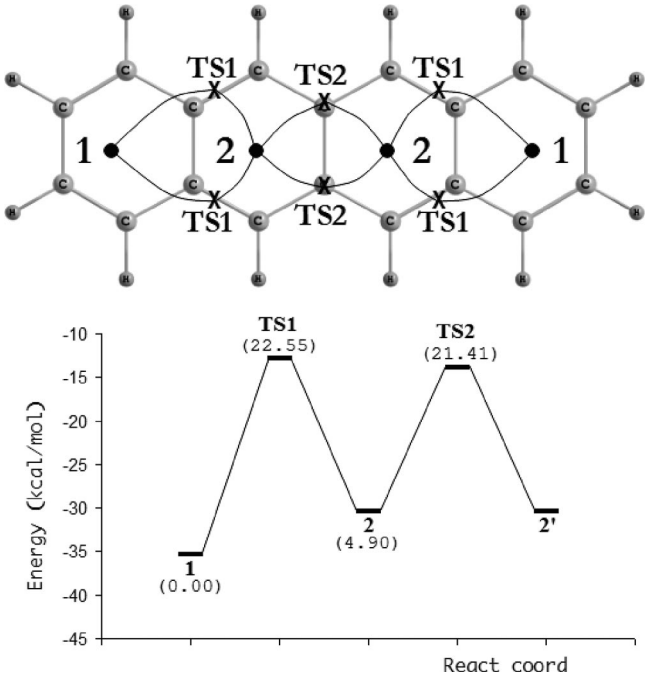

Figure 4. Sketched route for the haptotropic migrations in tetracene obtained at the B3LYP/(Watchers' basis/6-31G(d,p)) level of theory (top). The labels are marked in the outlined route as black circles for minima and × for transition states (TS). Relative energies with respect to species **1** (bottom) are given in parentheses. Energy scale in the *y* axis represents binding energies corrected by BSSE with respect to isolated $Cr(CO)_3$ and tetracene. All energies are given in kcal·mol^{-1}.

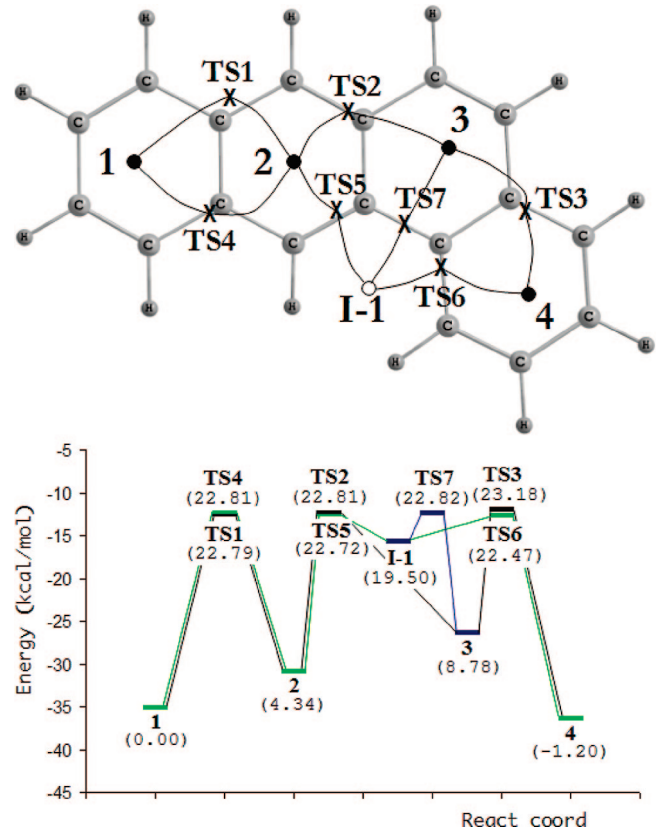

Figure 5. Sketched route for the haptotropic migrations in tetraphene obtained at the B3LYP/(Watchers' basis/6-31G(d,p)) level of theory (top). The labels are marked in the outlined route as black circles for minima and × for transition states (TS). Relative energies with respect to species **1** (bottom) are given in parentheses. Energy scale in the *y* axis represents binding energies corrected by BSSE with respect to isolated $Cr(CO)_3$ and tetraphene. All energies are given in kcal·mol^{-1}.

We discovered a more complex route for the haptomigration on the less symmetric tetraphene benzenoid. All minima and TSs involved in the IRHR in tetraphene are depicted in Figures 5 and S5 (see Supporting Information). Interestingly, the coordination position **4** is barely preferred than **1** by 1.2 kcal·mol^{-1}, whereas ring **3** is markedly unfavorable by 8.8 kcal·mol^{-1} with respect to **1**. These results, similar to that found in phenanthrene, are in line with experimental findings.[7] The existence of an intermediate connecting structures **2**, **3**, and **4** with energetic barriers of 18.4, 14.0, and 23.7 kcal·mol^{-1}, respectively, is expected from the fact that rings **2**, **3**, and **4** in tetraphene have the same shape as that found for the phenanthrene system. Even though there is not a clear selected route (*exo* vs *endo* side, the former being higher in energy by only about 1 kcal·mol^{-1}), once $Cr(CO)_3$ migrates from position **2** using the *endo* face, it can take a shorter path directly to **4** through **I-1**. This haptotropic path or the path through ring **3** can be indistinctly selected in the migration of the metallic complex, as it was already found for the (phenanthrene)$Cr(CO)_3$ complex.

Chrysene represents a more intriguing case as far as IRHR reaction mechanisms are concerned. The sketched routes and the associated structures for this energy diagram are shown in Figures 6 and S6 in the Supporting Information, respectively. The pathways are symmetric but present a different pattern from those presented above. Again, the more external rings (binding energy of −36.2 kcal·mol^{-1}) are preferred for the coordination of the tricarbonylchromium complex in comparison with the central rings (binding energy of −29.7 kcal·mol^{-1}).[7] It is noteworthy that at variance with the other studied kinked PAHs, for which an intermediate in the bay regions was found, for chrysene such intermediate is absent. Instead, there is a clear η^1-intermediate **I-1** connecting the haptotropic migration from ring **1** to ring **2** through transition states **TS1** and **TS2**. This *exo* reaction pathway is favored by just a few tenths of kcal·mol^{-1}.

Recently, we reported the haptotropic rearrangement of tricarbonylchromium over the two inner rings **2** of pyrene.[41] In Figure 7, the complete IRHR reaction mechanisms for this ligand are drawn. Precisely, the $Cr(CO)_3$ coordination on the less substituted ring **1** (binding energy of −32.3 kcal·mol^{-1}) is preferred over **2** by 5.5 kcal·mol^{-1}. Indeed, the experimental isolation of isomer **1** was achieved by Arrais and co-workers.[7] The presence of intermediate **I-1** was justified in our previous work[41] using molecular orbital arguments. There is also a direct inner pathway from ring **1** to **I-1** through a **TS3** structure, 3.8 kcal·mol^{-1} higher in energy than **TS1**, which again shows the greater preference of $Cr(CO)_3$ to move on the periphery of the PAH. Furthermore, as can be seen in Figure 7, the haptotropic rearrangement ring **1**−ring **2** rather than ring **2**−ring **2** is favored. The same conclusions were reached by the experimental and theoretical work of Howell et al.[43] The experimental energy barriers reported in that study (23 and 25 kcal·mol^{-1}) are in good agreement with ours, while their reported extended Hückel values were clearly underestimated.

The IRHR reaction mechanism in (triphenylene)$Cr(CO)_3$ species presents similar characteristics to those of phenanthrene. The energetic diagram and the scanned PES can be visualized in Figure 8, whereas the molecular structures corresponding to minima and TSs are shown in Figure S8 in the Supporting

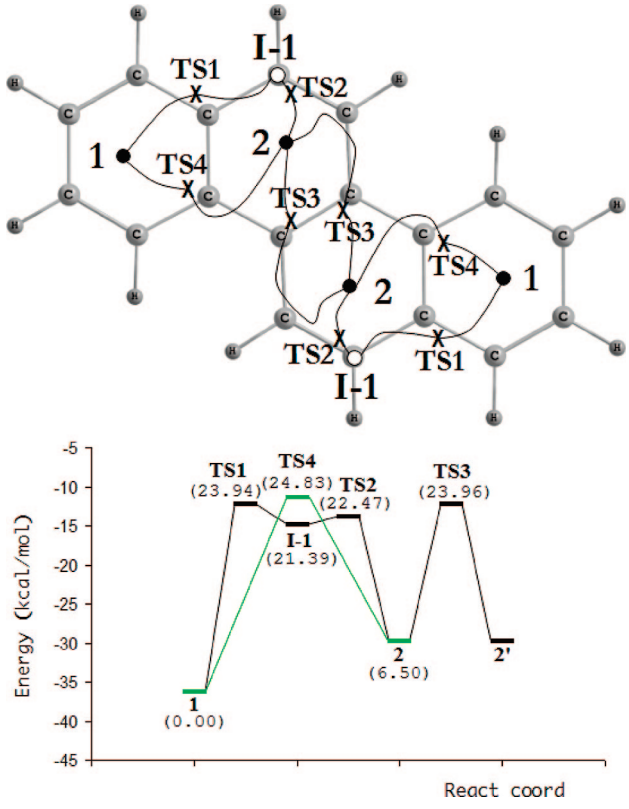

Figure 6. Sketched route for the haptotropic migrations in chrysene obtained at the B3LYP/(Watchers' basis/6-31G(d,p)) level of theory (top). The labels are marked in the outlined route as black circles for minima and × for transition states (TS). Relative energies with respect to species **1** (bottom) are given in parentheses. Energy scale in the *y* axis represents binding energies corrected by BSSE with respect to isolated $Cr(CO)_3$ and chrysene. All energies are given in kcal·mol^{-1}.

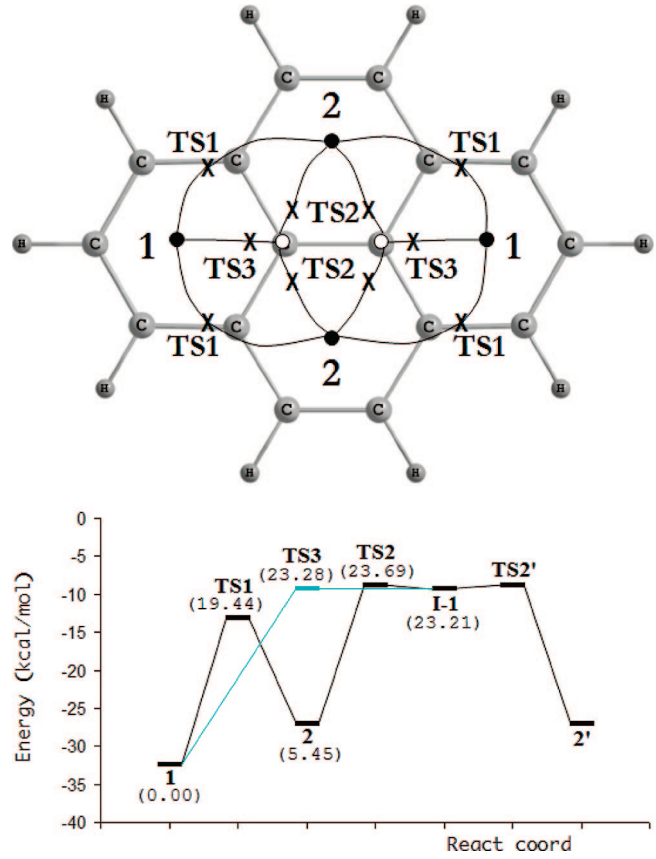

Figure 7. Sketched route for the haptotropic migrations in pyrene obtained at the B3LYP/(Watchers' basis/6-31G(d,p)) level of theory (top). The labels are marked in the outlined route as black/white circles for minima/intermediates and × for transition states (TS). Relative energies with respect to species **1** (bottom) are given in parentheses. Energy scale in the *y* axis represents binding energies corrected by BSSE with respect to isolated $Cr(CO)_3$ and pyrene. All energies are given in kcal·mol^{-1}.

Information. The binding energy of $Cr(CO)_3$ to triphenylene in **1** is −36.8 kcal·mol^{-1}. The position of the tricarbonylchromium coordinated at the central ring is quite high in energy (17.4 kcal·mol^{-1}, more than in the other isomer) as expected from the higher steric repulsion as well as the reduced π-electron density and low aromaticity of this central ring.[55] For this molecule, the presence of an η^4-intermediate similar to that found in phenanthrene in the bay regions is very clear. This bridge allows the outer rings **1** to avoid the more energetically demanding position **2** for haptotropic rearrangements. Our affirmations are supported by experimental work by Rogers et al.,[6] who also realized that the staggered *exo* orientation of (triphenylene)$Cr(CO)_3$, as we have found for all the structures reported here, is the common one for (benzenoid)$Cr(CO)_3$ complexes but not for (biphenylene)$Cr(CO)_3$ complexes (and the central rings of pyrene). Our calculated value for the activation barrier of 24.5 kcal·mol^{-1} in (triphenylene)$Cr(CO)_3$ is lower than that found experimentally in the (fluoranthene)$Cr(CO)_3$ species (32.6 kcal·mol^{-1}), which possess a central cyclopentadienyl ring instead of benzene and has a condensed naphthalene fragment on one side.[56]

Finally, we present the case of tetrahelicene, a helicoidal benzenoid of four fused 6-MRs, which to our best knowledge has not been reported yet complexed with tricarbonylchromium. Figure 9 shows the scanned PES and the energy barriers for the elucidated reaction mechanisms (minima and TS structures can be visualized in Figure S9, Supporting Information). Also here we see that the preferred coordination sites of $Cr(CO)_3$ are the outer rings **1** and **4**. The binding energy of the $Cr(CO)_3$ to tetrahelicene in **1** is −35.6 kcal·mol^{-1}, only 0.6 kcal·mol^{-1} higher than that in chrysene. Both π-faces are symmetrical and the order of the rings can be inverted in the sketched PES to obtain the binding energies for the coordination to the other face (Scheme 1 indicates the face studied). The more congested *endo* pathway of tetrahelicene presents higher steric hindrance, and this can be the reason why the *exo* haptomigration is clearly more favored. Looking at the activation barriers, we can deduce that the energy differences of 1−3 kcal·mol^{-1} between both reaction pathways induce a significant selectivity in the mechanism of IRHR for tetrahelicene. The discovered intermediate (**I-1**) found for the haptotropic rearrangement between rings **2** and **3** (*endo* side) through **TS5** and **TS6** is an η^2-coordinated species. The values of the shortest Cr−C bond distances in this intermediate (going downhill in the twist) are 2.69, 2.41, 2.25, 2.73, and 3.50 Å. In this species, we have found a different kind of haptotropic migration not described before. In this unprecedented mechanism (see Figure 10) the tricarbonylchromium unit moves from the central ring **2** to an intermediate (**Int**) followed by the inversion of the tetrahelicene helix, which

(55) Matito, E.; Duran, M.; Solà, M. *J. Chem. Phys.* **2005**, *122*, 014109; erratum, **2006**, *125*, 059901.

(56) Oprunenko, Y.; Malyugina, S.; Vasil'ko, A.; Lyssenko, K.; Elschenbroich, C.; Harms, K. *J. Organomet. Chem.* **2002**, *641*, 208.

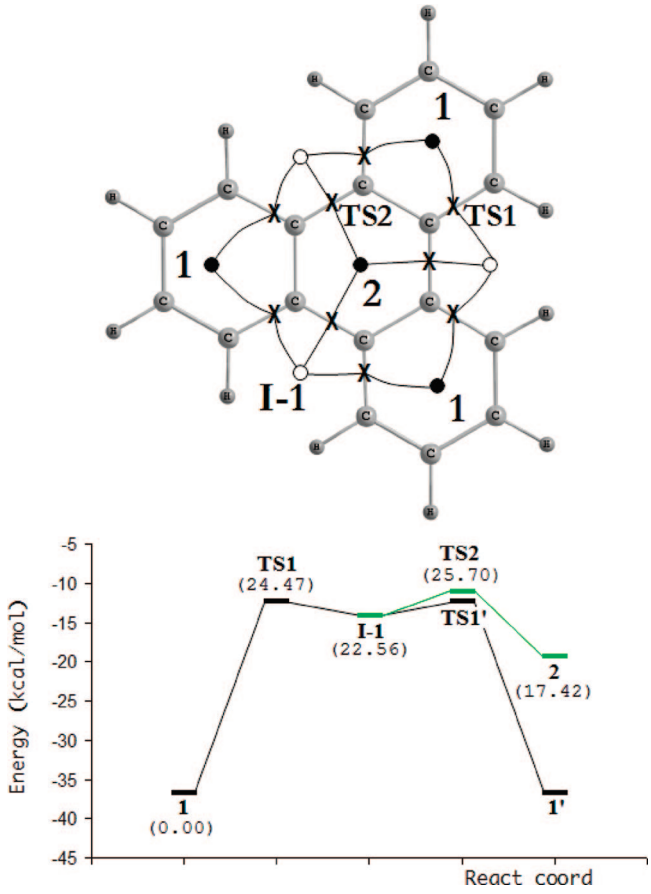

Figure 8. Sketched route for the haptotropic migrations in triphenylene obtained at the B3LYP/(Watchers' basis/6-31G(d,p)) level of theory (top). The labels are marked in the outlined route as black circles for minima and × for transition states (TS). Relative energies with respect to species **1** (bottom) are given in parentheses. Energy scale in the *y* axis represents binding energies corrected by BSSE with respect to isolated $Cr(CO)_3$ and triphenylene. All energies are given in kcal·mol^{-1}.

undergoes an *R* to *S* enantiomeric transformation. The η^4-intermediate involved in this migration (**Int**) has a substantially different degree of hapticity than the previously mentioned η^2-intermediate (**I-1**), with Cr−C distances of 2.36, 2.47, 2.38, 2.54, and 3.02 Å, and with a position more centered on the *endo* carbon atoms. The geometrical structures of this haptotropic inversion mechanism are depicted in Figure 11. Unfortunately, we cannot say this reaction mechanism is in competition with the others localized in Figure 9. Whereas the "normal" haptotropic rearrangement from ring **2** to ring **3** requires 15.3 kcal·mol^{-1}, this pathway involves barriers of 16.5 kcal·mol^{-1} (for the coordination mode in **Int**, Figures 10 and 11) and 35.4 kcal·mol^{-1} (inversion of (*R*)-tetrahelicene to (*S*)-tetrahelicene) = 51.5 kcal·mol^{-1}, relative to ring **2**.

We have investigated the aromatic character of the benzenoid π-ligands presented here before and after tricarbonylchromium coordination. In order to achieve this, we have used some of the most generally accepted aromaticity indices.[57] The results are given also in the Supporting Information (Tables S1−S9). Previous work discussing local aromaticity in some of these

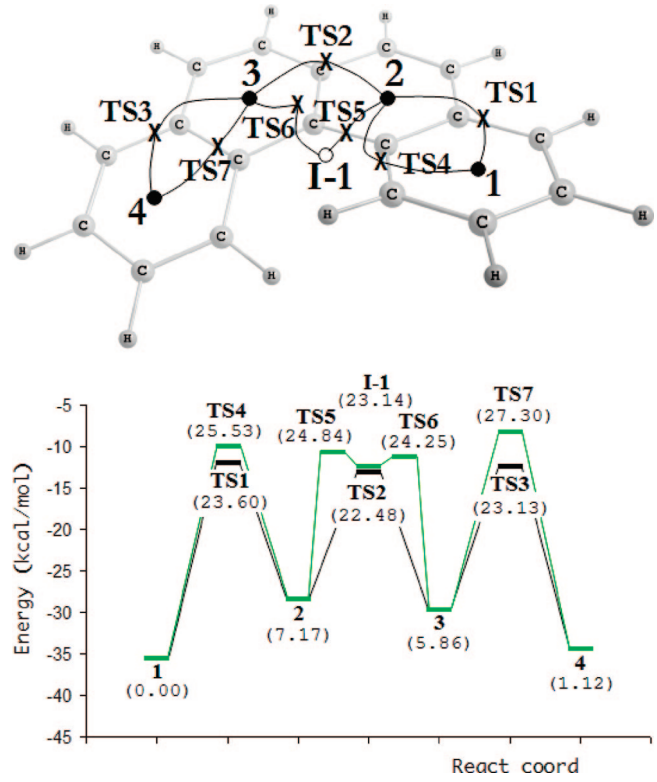

Figure 9. Sketched route for the haptotropic migrations in tetrahelicene obtained at the B3LYP/(Watchers' basis/6-31G(d,p)) level of theory (top). The labels are marked in the outlined route as black/white circles for minima/intermediates and × for transition states (TS). Relative energies with respect to species **1** (bottom) are given in parentheses. Energy scale in the *y* axis represents binding energies corrected by BSSE with respect to isolated $Cr(CO)_3$ and tetrahelicene. All energies are given in kcal·mol^{-1}.

systems has been published by our group.[39,50,58] In general, we can say that in these species aromaticity measurements derived from electronic and magnetic criteria correlate quite well. They predict that the central rings in linear acenes are slightly more aromatic than the outer ones, whereas for the angular PAHs and tetrahelicene the more aromatic rings are the external ones. The coordination of $Cr(CO)_3$ reduces the aromaticity in the coordinated ring.[59] We have verified that this change also affects the neighboring rings but far less than the coordinated ring. For the case of tetraphene, the coordination of tricarbonylchromium in one extreme of the molecule enhances slightly the aromaticity in the more distant ring. The same observations in local aromaticity changes are drawn for PAHs complexed with the lithium cation.[39]

In general, we have observed that similar IRHR pathways are found for acenes having a common skeleton. Thus, (naphthacene)$Cr(CO)_3$ haptomigration pathway has the same characteristics as that found in (anthracene)$Cr(CO)_3$ or (naphthalene)$Cr(CO)_3$. Benzenoid ligands such as tetraphene, triphenylene, and to some extent tetrahelicene share a common structure with phenanthrene, and all of them have similar energy requirements for the *exo* and *endo* pathways and present an η^2-intermediate in the bay region. (Chrysene)$Cr(CO)_3$, however, does not show the same behavior because its more significant π-HOMOs

(57) For the methodology used here and the references of the methods used for measuring aromaticity, please see ref 41.

(58) Portella, G.; Poater, J.; Solà, M. *J. Phys. Org. Chem.* **2005**, *18*, 785.

(59) Feixas, F.; Jimenez-Halla, J. O. C.; Matito, E.; Poater, J.; Solà, M. *Polish J. Chem.* **2007**, *81*, 783.

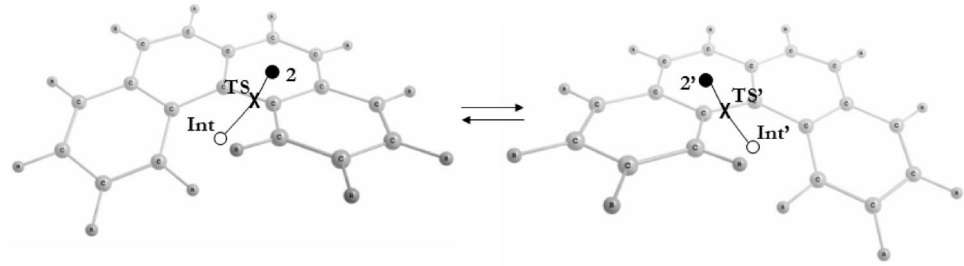

Figure 10. Haptotropic inversion mechanism found for the (tetrahelicene)$Cr(CO)_3$ complex on an inner (second) ring.

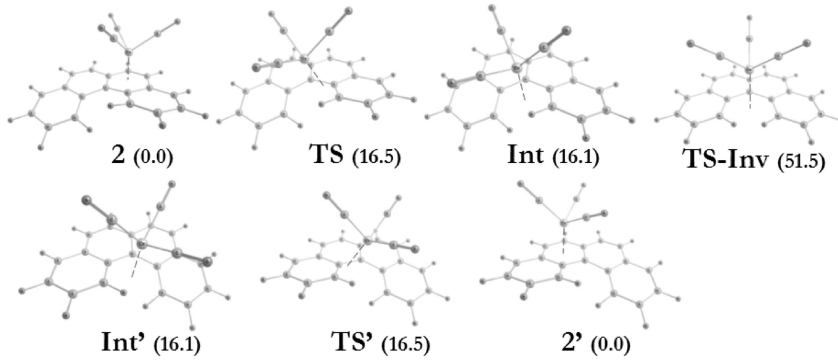

Figure 11. Optimized structures for an alternative route of $Cr(CO)_3$ haptomigration found on the tetrahelicene ligand. Relative energies with respect to minimum **2** are given in kcal·mol^{-1}.

interactions are contained at the *exo* carbons, where tricarbonylchromium forms the η^1-intermediate shown in Figure S6, Supporting Information. For fused PAHs bearing an η^4-intermediate, we find the existence of an early η^2-TS in a position located closer to the reactant than to the intermediate along the reaction path. For those kinked PAHs not having such an η^4-intermediate, there is an η^3-TS connecting the outer and inner rings. Moreover, our results suggest that PAHs with three fused 6-MRs sharing a common C atom have an η^1-intermediate located at that shared C atom. This situation is, however, less favored than haptomigrations through the periphery of these systems. In particular, we also point out that the effect on the curvature of the arene ligands[41] can transform this intermediate into a TS. This is because transient stable interactions with the neighboring carbons of the methylene carbon fragment become lost if the arene bends out. In Scheme 4, we summarize the results obtained in this work.

Whether some experiments have been reported supporting our results or have been carried out only for certain derivative systems and substituted isomers, the tricarbonylchromium unit is always found bonded to a terminal rather than to a central ring of PAHs. This was suggested a long time ago,[60] arguing that the electron-withdrawing character of $Cr(CO)_3$ anchors the metallic complex to the ring richer in electrons. What is more, Own and co-workers[61] reported on a series of substituted linear and angular PAHs complexed with tricarbonylchromium. They found that in most cases the terminal ring position was favored for coordination, but by modifying the total π-electron density of PAHs one can habilitate the $Cr(CO)_3$ complexation in the other rings.

(60) Nicholson, B. J. *J. Am. Chem. Soc.* **1966**, *88*, 5156.
(61) Own, Z. Y.; Wang, S. M.; Chung, J. F.; Miller, D. W.; Fu, P. P. *Inorg. Chem.* **1993**, *32*, 152.

Conclusions

In this work, we have discussed the reaction mechanisms of IRHRs in all PAHs with three and four 6-MRs. All possible ways by which haptomigrations can occur have been explored and, for the less symmetric PAHs, nonequivalent reaction pathways were discerned. It is found that the metal complex prefers to be coordinated on the less substituted rings (usually the more aromatic ones and with the higher π-density) and tends to avoid migration to the more substituted ring. This is especially apparent in the case of triphenylene, where the coordination with the outer rings is 17.4 kcal·mol^{-1} more favored than with the inner ring.

Some highlights can be drawn from the scanned potential energy surfaces explored: (1) the number of condensed aromatic rings entails not only a decrease in the binding energy associated with metal coordination but also a reduction of the IRHR activation barriers (*i.e.*, for linear benzenoids, IRHRs become more favorable in the series naphthalene < anthracene < tetracene); (2) linear arenes undergo easier haptotropic rearrangements than their angular counterparts due to the reduced homogeneity of electron density of the latter; (3) the π-HOMOs of every PAH studied and the condition of whether the coordinated ring is in a terminal or inner position seem to determine the possible reaction mechanism by which haptomigration occurs. In other words, the position of transition states (perfect η^3-species or late transient structures) and the existence of an intermediate are influenced by both mentioned factors.

For the case of haptotropic reactions over the surface of tetrahelicene, we found a more pronounced selection of intramolecular migrations because of inherent steric repulsions produced by its helicoidal shape. A different route consisting of an inversion of the ligand assisted by haptotropic movement was found in this system. However, the barrier reaction for the IRHR and the transition state for the (*R*,*S*)-enantiomeric

Scheme 4. Summary of the Different Reaction Pathways for the Intramolecular Inter-ring Haptotropic Rearrangements Analyzed in This Work

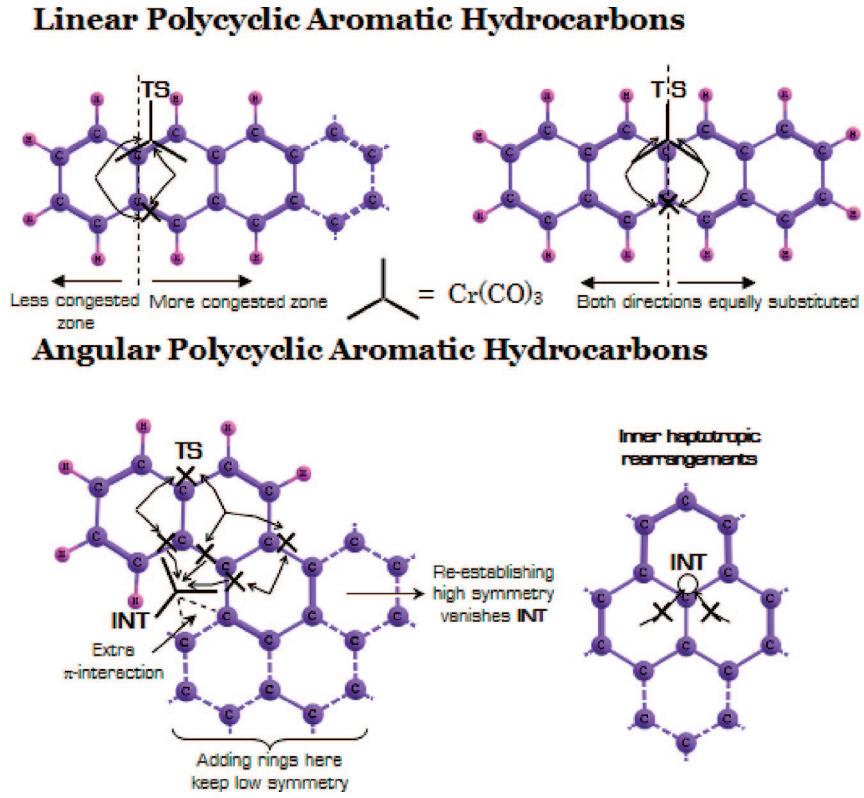

transformation are quite high in energy to compete with the other haptotropic reactions.

Computational Details

Geometry optimizations were performed by using Becke's nonlocal three-parameter exchange functional[62] and the gradient-corrected Lee−Yang−Parr correlation functional,[63] the so-called B3LYP hybrid functional, implemented in the Gaussian03[64] program package. For our study, such a well-known functional is quite suitable, as the organometallic complexes involved in the haptotropic rearrangement have been shown to possess single reference character.[42] As to the basis set, the addition of polarization functions has been shown to be important to correctly describe the Cr−arene interaction in these kinds of complexes studied.[46] For this reason, we employed the polarized 6-31G(d,p)[65,66] basis set for C, O, and H atoms and the Wachters (14s9p5d3f)/(8s4p3d1f) basis set with polarization functions for chromium[67] using the expanded contraction scheme (62111111/3312/311/3). We denoted this mixed basis set as Wachters' basis/6-31G(d,p) throughout this work. Relativistic effects are unimportant for accurate calculations of chromium complexes[68] and were neglected in our calculations. Finally, since actual experiments are typically carried out in rather nonpolar solvents, solvent effects are small[49] and have not been considered in our study.

We also performed harmonic vibrational frequency calculations to verify the nature of the critical points on the PES. The number of negative frequencies must be zero for minima and one for any true TS. We also made sure that the imaginary frequency effectively connects both minima sides through intrinsic-reaction-coordinate calculations. Binding energies were corrected by adding the zero-point energy (ZPE) and the basis set superposition error (BSSE) in the critical points of the PES according to the following expression:

$$\Delta E = \Delta E_{\mathrm{el}} + \mathrm{ZPE(AB)} - \mathrm{ZPE(A)} - \mathrm{ZPE(B)} + \delta^{\mathrm{BSSE}} \quad (1)$$

where $\Delta E_{el} = E_{\mathrm{AB}}^{\mathrm{AB}}(\mathrm{AB}) - E_{\mathrm{A}}^{\mathrm{A}}(\mathrm{A}) - E_{\mathrm{B}}^{\mathrm{B}}(\mathrm{B})$. Here $E_Y^Z(X)$ represents the energy of subsystem X at optimized geometry Y using the basis set Z and the counterpoise correction is defined as[69,70]

$$\delta^{\mathrm{BSSE}} = E_{\mathrm{AB}}^{\mathrm{A}}(\mathrm{A}) + E_{\mathrm{AB}}^{\mathrm{B}}(\mathrm{B}) - E_{\mathrm{AB}}^{\mathrm{AB}}(\mathrm{A}) - E_{\mathrm{AB}}^{\mathrm{AB}}(\mathrm{B}) \quad (2)$$

In our work, we found this energy correction has an average value of 3.9 kcal·mol^{-1} for the studied systems. Figures of the

(62) Becke, A. D. *J. Chem. Phys.* **1993**, *98*, 5648.
(63) Lee, C. T.; Yang, W. T.; Parr, R. G. *Phys. Rev. B* **1988**, *37*, 785.
(64) Frisch, M. J.; Trucks, G. W.; Schlegel, H. B.; Scuseria, G. E.; Robb, M. A.; Cheeseman, J. R., Jr.; Vreven, T.; Kudin, K. N.; Burant, J. C.; Millam, J. M.; Iyengar, S. S.; Tomasi, J.; Barone, V.; Mennucci, B.; Cossi, M.; Scalmani, G.; Rega, N.; Petersson, G. A.; Nakatsuji, H.; Hada, M.; Ehara, M.; Toyota, K.; Fukuda, R.; Hasegawa, J.; Ishida, M.; Nakajima, T.; Honda, Y.; Kitao, O.; Nakai, H.; Klene, M.; Li, X.; Knox, J. E.; Hratchian, H. P.; Cross, J. B.; Adamo, C.; Jaramillo, J.; Gomperts, R.; Stratmann, R. E.; Yazyev, O.; Austin, A. J.; Cammi, R.; Pomelli, C.; Ochterski, J.; Ayala, P. Y.; Morokuma, K.; Voth, G. A.; Salvador, P.; Dannenberg, J. J.; Zakrzewski, V. G.; Dapprich, S.; Daniels, A. D.; Strain, M. C.; Farkas, O.; Malick, D. K.; Rabuck, A. D.; Raghavachari, K.; Foresman, J. B.; Ortiz, J. V.; Cui, Q.; Baboul, A. G.; Clifford, S.; Cioslowski, J.; Stefanov, B. B.; Liu, G.; Liashenko, A.; Piskorz, P.; Komaromi, I.; Martin, R. L.; Fox, D. J.; Keith, T.; Al-Laham, M.; Peng, C.; Nanayakkara, A.; Challacombe, M.; Gill, P. M. W.; Johnson, B. G.; Chen, W.; Wong, M. W.; González, C.; Pople, J. A. *Gaussian 03, rev. B03*; Pittsburgh, PA, 2003.
(65) Francl, M. M.; Pietro, W. J.; Hehre, W. J.; Binkley, J. S.; Gordon, M. S.; Defrees, D. J.; Pople, J. A. *J. Chem. Phys.* **1982**, *77*, 3654.
(66) Hariharan, P. C.; Pople, J. A. *Theor. Chim. Acta* **1973**, *28*, 213.
(67) Wachters, A. J. *J. Chem. Phys.* **1970**, *52*, 1033.
(68) Jacobsen, H.; Schreckenbach, G.; Ziegler, T. *J. Phys. Chem.* **1994**, *98*, 11406.
(69) Boys, S. F.; Bernardi, F. *Mol. Phys.* **1970**, *19*, 553.
(70) Salvador, P.; Duran, M. *J. Chem. Phys.* **1999**, *111*, 4460.

molecular geometries were generated by using the ChemCraft visualization program.[71]

Acknowledgment. Financial help has been furnished by the Spanish Ministerio de Educación y Ciencia (MEC) projects no. CTQ2005-08797-C02-01/BQU and CTQ2008-03077/BQU and by the Catalan Departament d'Universitats, Recerca i Societat de la Informació (DURSI) of the Generalitat de Catalunya project no. 2005SGR-00238. J.O.C.J.-H. acknowledges the DURSI of Generalitat de Catalunya and the European Social Fund for financial support through Doctoral Fellowship 2005FI/00451 and Dr. Pedro Salvador for useful comments in this work. The authors thank the Centre de Supercomputació de Catalunya (CESCA) for providing partial computer time.

Supporting Information Available: Optimized Cartesian *xyz* coordinates of all stationary points located on the PES for each reaction mechanism studied here as well as figures showing all critical points of the explored PES and tables collecting all aromaticity measurements calculated for all structures studied in this work. This material is available free of charge via the Internet at http://pubs.acs.org.

OM800505J

(71) Zhurko, G. A.; Zhurko, D. A. *ChemCraft v. 1.5*; http://www.chemcraftprog.com.